Influence of temperature on molecular interactions of imidazolium-based ionic liquids with acetophenone: Thermodynamic properties and quantum chemical studies

Article *in* RSC Advances · November 2016
DOI: 10.1039/C6RA15476J

CITATION
1

READS
41

4 authors:

Indra Bahadur
University of KwaZulu-Natal
112 PUBLICATIONS **1,015** CITATIONS
SEE PROFILE

Kgomotso Masilo
North West University South Africa
1 PUBLICATION **1** CITATION
SEE PROFILE

Eno Ebenso
North West University South Africa
145 PUBLICATIONS **1,244** CITATIONS
SEE PROFILE

Gan Redhi
Durban University of Technology
40 PUBLICATIONS **429** CITATIONS
SEE PROFILE

RSC Advances

PAPER

View Article Online
View Journal | View Issue

Cite this: *RSC Adv.*, 2016, **6**, 104708

Influence of temperature on molecular interactions of imidazolium-based ionic liquids with acetophenone: thermodynamic properties and quantum chemical studies†

Indra Bahadur,*[a] Masilo Kgomotso,[a] Eno E. Ebenso[a] and Gan Redhi[b]

The physicochemical properties namely: densities (ρ), sound velocities (u), viscosities (η), and refractive indices (n_D) of a series of alkyl imidazolium-based ionic liquids (ILs) with same cation and different anion and *vice versa* of ILs: 1-butyl-3-methylimidazolium tetrafluoroborate $[BMIM]^+[BF_4]^-$, 1-butyl-3-methylimidazolium hexafluorophosphate $[BMIM]^+[PF_6]^-$, 1-ethyl-3-methylimidazoium ethyl sulphate $[EMIM]^+[EtSO_4]^-$ and 1-ethyl-3-methylimidazolium tetrafluoroborate $[EMIM]^+[BF_4]^-$, with acetophenone over the wide range of composition and at (293.15, 303.15, 313.15, 323.5 and 333.15) K under atmospheric pressure is reported in this study. The excess molar volumes, (V^E_m), deviation in isentropic compressibilities ($\Delta\kappa_s$), deviation in viscosities ($\Delta\eta$) and deviation in refractive indices (Δn_D) were derived from experimental results. The V^E_m, $\Delta\kappa_s$ and Δn_D values for the mentioned systems are both negative and positive over the entire composition range while the $\Delta\eta$ values are negative under the same experimental conditions. The derived properties were fitted to the Redlich–Kister polynomial equation to check the accuracy of experimental results. Furthermore, the inter-ionic interactions between the cations and anions of the ILs both *in vacuo* and in acetophenone (using continuum solvation) were confirmed using quantum chemical technique such as [Density Functional Theory (DFT)]. The quantum chemical results are in good agreement with the experimental results suggesting that there exist appreciable interactions between the ILs and acetophenone. The theoretical and measured data were interpreted in terms of intermolecular interfaces and structural effects between similar and dissimilar molecules upon mixing in order to obtain more information on the thermophysical and thermodynamic properties of ILs and their binary mixtures. This study will contribute to the data bank of thermodynamic properties of IL mixtures, so as to establish principles for the molecular design for chemical separation processes and to enhance the applications of ILs in certain aspects of research or industrial application.

Received 14th June 2016
Accepted 26th October 2016

DOI: 10.1039/c6ra15476j

www.rsc.org/advances

1. Introduction

Ionic liquid (IL) is a term which is used to describe a broad group of salts which have an extensive liquid range.[1] This includes organic or inorganic molten salts, fused salts, non-aqueous ILs and liquid organic salts.[2,3] As compared to traditional molecular solvents, ILs are liquids at ambient temperatures and are composed entirely of ions referring to cations and anions, and are held together by columbic forces.[4–6] The melting point of ILs is relatively low and/at below 100 °C, therefore they remain as liquids within a broad temperature window.[1–4] The low melting point of ILs is due to its chemical composition,[7,8] the relatively large size of either the anion or the cation in ILs and low symmetry which also explains the lower melting points of these ILs.[1] ILs that melt at room temperature are said to be room temperature ionic liquids (RTILs).[9] The ILs possess more favourable properties than organic molecular solvents, which includes broad liquid range, negligible vapour pressure therefore most unlikely to evaporate under normal conditions, high thermal stability, non-flammable and found to be stable at room temperature.[3,10,11] ILs have high polarity, miscible and soluble with water and other organic solvents.[3,7] Ionic interaction within ILs enables them to be miscible with polar substances, miscibility with water and organic solvents depends on the side chain lengths on the cation and the anion combinations,[8,10] and also allows a large variety of interactions and applications.[12–14]

[a]*Department of Chemistry and Materials Science Innovation, Modelling Research Focus Area, School of Mathematical and Physical Sciences, Faculty of Agriculture, Science and Technology, North-West University (Mafikeng Campus), Private Bag X2046, Mmabatho 2735, South Africa. E-mail: bahadur.indra@gmail.com; bahadur.indra@nwu.ac.za; Tel: +27 18 389 2870*

[b]*Department of Chemistry, Durban University of Technology, P O Box 1334, Durban, 4000, South Africa*

† Electronic supplementary information (ESI) available. See DOI: 10.1039/c6ra15476j

Acetophenone is an important industrial chemical, widely used as an ingredient of flavour and fragrance in soaps, detergents, cosmetics creams, lotions, and perfumes.[15] It has also been used as an important intermediate for pharmaceuticals and agrochemicals.[15] Furthermore, it is used as a plasticizer, as a solvent in resins, for cellulose ethers, as a hypnotic (induces sleep),[16] in organic syntheses as a photosensitizer and as a catalyst for the polymerization of olefins.[17] The thermodynamic properties of systems containing acetophenone are helpful to better understand molecular interaction and to design and simulate the different processes of separation.[15] Unlike other ketones like acetone and 2-pyrrolidone, acetophenone can be used for medical purposes in, whereby it can be used to kill cancer cell. In comparison to simple alcohol like methanol, acetophenone play a role in animal metabolite whereas methanol plays a role in bacterial metabolite.

The thermophysical and thermodynamics properties of ILs mixtures allow for new correlations and/or predictive models to test the solution theories for ILs and their binary mixtures with organic solvents[18–25] as well as provide information about molecular interactions such as solute–solute, solute–solvent and solvent–solvent that occur in binary mixtures specifically where hydrogen bonding takes place. Thus a more systematic study of thermodynamic and thermophysical properties of ILs and their mixtures with solvents is required in chemical and separation processes. Furthermore, accurate knowledge about the thermophysical and thermodynamic data is critical in order to transfer the ILs from laboratory to industry, designing future processes and equipment involving these ionic compounds.[26–30]

Density Functional Theory (DFT)[31] (a quantum chemical method) focuses on the electron density of the system, which depends on only three variables. DFT method have turned out to be exceptionally well known recently because of their accuracy that is similar to other techniques in less time and with a smaller investment from the computational perspective. In most recent years, theoretical quantum chemical calculations have turn out to be complementary for experimental methods in many fields.[32–44]

The volumetric, acoustic and transport properties of liquids and liquid mixtures are utilised to study the molecular interactions between the several components of the mixtures[45] and also to understand engineering applications concerning heat transfer, mass transfer and fluid flow. Thus, data on some of the properties associated with the liquids and liquid mixtures such as density, viscosity, sound velocity and refractive index find extensive application in solution theory and molecular dynamics. Such results are essential for elucidation of data obtained from thermochemical, electrochemical, biochemical and kinetic studies. To the best of our knowledge, few work has been done on studied ILs with other solvents in literature (Rao *et al.*;[46] Zafarani-Moattar and Shekaari;[47] González *et al.*[48] and Bhagour *et al.*[49]) but no literature data are available in literature on thermophysical or thermodynamics properties of these ionic liquids under study in acetophenone with quantum chemical calculation. This therefore emphasises the novelty of the present investigation.

In the present work, a new inclusive record for the density, sound velocity, viscosity, and refractive index, of alkyl imidazolium based ionic liquids, which include 1-butyl-3-methylimidazolium tetrafluoroborate $[BMIM]^+[BF_4]^-$, 1-butyl-3-methylimidazolium hexafluorophosphate $[BMIM]^+[PF_6]^-$, 1-ethyl-3-methylimidazoium ethyl sulphate $[EMIM]^+[EtSO_4]^-$, 1-ethyl-3-methylimidazolium tetrafluoroborate $[EMIM]^+[BF_4]^-$, and their binary mixture with acetophenone at various temperatures and concentrations together with quantum chemical calculation is introduced. The results are used to derive other thermodynamic data namely; excess molar volume, deviation in isentropic compressibility, deviation in refractive indexes and deviation in viscosity. The intermolecular interactions in the ILs and their binary mixtures were evaluated. Furthermore, the influence in temperature and concentration, as well as the variance in the anion, cation and alkyl group of the IL and their binary mixtures were discussed. The present work is a part of the comprehensive and extensive investigations on-going in our research group on physicochemical properties of alkyl imidazolium/ammonium-based ILs with solvents at different temperatures and incorporation of the quantum chemical studies to support experimental data.[50–61]

2. Experimental procedure

2.1. Materials

Imidazolium based ILs used in the present study namely 1-butyl-3-methylimidazolium tetra fluoroborate $[BMIM]^+[BF_4]^-$, 1-butyl-3-methylimidazolium hexafluorophosphate $[BMIM]^+[PF_6]^-$ and 1-ethyl-3-methylimidazolium tetra fluoroborate $[EMIM]^+[BF_4]^-$ were obtained from Ionic Liquids Technologies Inc., 1-ethyl-3-methylimidazoium ethyl sulphate $[EMIM]^+[EtSO_4]^-$ was purchased from Sigma-Aldrich with the purity of ≥98%. The solvent acetophenone was supplied by Sigma-Aldrich. Deionised water was used in the experiments. The purity and the investigated thermophysical properties of acetophenone and ILs are presented in Table 1 together with literature[62–66] reported at 303.15 K. The mass percent water content was determined using

Table 1 Pure component specifications: suppliers, molecular weight (MW), specified purity and density at 303.15 K and at pressure $p = 0.1$ MPa

Solvent	Supplier	MW/g mol^{-1}	% purity	ρ/g cm^{-3}
$[BMIM]^+[BF_4]^-$	Ionic Liquids Technologies Inc.	226.022	99	1.20129 (ref. 62)
$[BMIM]^+[PF_6]^-$	Ionic Liquids Technologies Inc.	284.182	99	1.36240 (ref. 63)
$[EMIM]^+[BF_4]^-$	Ionic Liquids Technologies Inc.	197.970	98	1.28174 (ref. 64)
$[EMIM]^+[EtSO_4]^-$	Sigma-Aldrich	236.289	≥98	1.23425 (ref. 65)
Acetophenone	Sigma-Aldrich	120.148	>99	1.01942 (ref. 66)

Table 2 Coefficients A_i, and standard deviations, σ, obtained for the binary systems {$[BMIM]^+[BF_4]^-$ or $[BMIM]^+[PF_6]^-$ or $[EMIM]^+[BF_4]^-$ or $[EMIM]^+[EtSO_4]^-$ (x_1) + acetophenone (x_2)} at different temperatures and at pressure $p = 0.1$ MPa for the Redlich–Kister equation

	T/K	A_0	A_1	A_2	A_3	A_4	σ
{$[BMIM]^+[BF_4]^-$ (x_1) + acetophenone (x_2)}							
V_m^E/cm^3 mol^{-1}	293.15	18.852	−0.637	−3.972	−1.029	0.131	0.106
	303.15	19.631	−0.803	−4.373	−3.110	3.022	0.103
	313.15	20.449	−1.587	−6.059	−4.431	8.210	0.113
	323.15	21.333	−1.755	−6.516	−7.050	11.654	0.119
	333.15	22.574	−2.933	−13.007	−9.821	22.630	0.170
$\Delta\kappa_s$/TPa^{-1}	293.15	237 330	−22 924	37 085	89 050	44 842	543
	303.15	233 685	−20 053	24 521	99 867	11 297	411
	313.15	225 243	−18 744	25 051	111 467	−44 855	831
	323.15	214 378	−32 887	34 326	146 457	−104 398	644
	333.15	203 168	−320 638	217 978	1 486 978	−1 228 338	1373
$\Delta\eta$/mPa s	293.15	−131.150	136.112	−70.256	466.800	−482.503	0.786
	303.15	−72.971	51.551	−47.655	248.928	−191.642	0.436
	313.15	−59.012	39.132	25.249	168.289	−202.855	1.134
	323.15	−37.538	14.851	14.935	125.530	−133.040	0.537
	333.15	−25.400	13.596	34.790	90.037	−133.621	0.839
Δn	293.15	−0.0560	−0.0085	−0.0128	−0.0697	0.1364	0.0002
	303.15	−0.0552	−0.0192	0.0022	−0.0415	0.1291	0.0002
	313.15	−0.0510	−0.0209	−0.0051	−0.0416	0.1159	0.0003
	323.15	−0.0474	−0.0249	−0.0077	−0.0349	0.1213	0.0004
	333.15	−0.0443	−0.0242	0.0211	−0.0349	0.1100	0.0004
{$[BMIM]^+[PF_6]^-$ (x_1) + acetophenone (x_2)}							
V_m^E/cm^3 mol^{-1}	293.15	25.867	−19.539	−13.925	−5.802	17.259	0.058
	303.15	26.252	−19.848	−14.239	−6.323	18.098	0.060
	313.15	26.668	−20.117	−14.717	−7.167	19.465	0.062
	323.15	27.111	−20.513	−14.953	−7.661	20.216	0.065
	333.15	27.629	−20.878	−15.365	−8.669	21.732	0.069
$\Delta\kappa_s$/TPa^{-1}	293.15	169 167	−254 159	−217 659	−58 317	92 919	656
	303.15	169 169	−254 157	−217 677	−58 338	92 944	656
	313.15	138 325	−290 681	−137 488	57 475	−64 931	610
	323.15	115 907	−259 106	−185 707	−213	−50 674	998
	333.15	87 080	−306 315	−225 102	151 424	−95 946	983
$\Delta\eta$/mPa s	293.15	−352.733	273.914	−283.830	959.770	−847.274	2.253
	303.15	−204.106	110.791	−83.038	637.389	−652.417	2.346
	313.15	−110.457	54.423	−77.853	323.853	−272.339	0.794
	323.15	−67.379	19.187	−13.282	214.549	−217.628	0.915
	333.15	−43.425	17.276	29.925	139.596	−211.452	0.928
Δn	293.15	−0.1436	−0.0381	0.0072	0.0221	0.0241	0.0002
	303.15	−0.0479	−0.0154	0.0554	−0.0678	0.0526	0.0004
	313.15	−0.0455	−0.0195	0.0534	−0.0686	0.0716	0.0005
	323.15	−0.0396	−0.0178	0.0443	−0.0757	0.0959	0.0005
	333.15	−0.0365	−0.0181	0.0681	−0.0841	0.0657	0.0003
{$[EMIM]^+[BF_4]^-$ (x_1) + acetophenone (x_2)}							
V_m^E/cm^3 mol^{-1}	293.15	7.762	−21.213	4.294	−4.592	6.467	0.056
	303.15	10.164	−21.110	1.146	−12.883	15.145	0.113
	313.15	10.587	−21.508	0.805	−14.441	17.417	0.125
	323.15	11.046	−21.924	0.418	−16.138	19.923	0.140
	333.15	11.393	−22.981	3.878	−18.262	18.181	0.155
$\Delta\kappa_s$/TPa^{-1}	293.15	261 467	−238 721	−123 000	−234 443	264 715	1010
	303.15	220 921	−167 349	−133 613	−134 309	8675	794
	313.15	182 119	−172 264	−155 579	−23 923	−39 482	521
	323.15	143 344	−135 284	−81 811	−41 407	−200 615	793
	333.15	121 550	−182 071	−169 015	925	−98 418	1058
$\Delta\eta$/mPa s	293.15	−43.545	28.300	−48.306	89.442	−62.857	0.112
	303.15	−27.540	12.528	−11.914	59.761	−63.258	0.195
	313.15	−18.761	12.249	−8.344	34.175	−40.769	0.193
	323.15	−13.309	11.7670	−14.720	20.466	−16.561	0.135
	333.15	−8.046	2.827	−7.386	10.065	−5.082	0.119
Δn	293.15	−0.0302	−0.0235	0.0974	−0.0083	−0.0432	0.0002
	303.15	−0.0272	−0.0256	0.0949	0.0086	−0.0374	0.0003

Table 2 (*Contd.*)

	T/K	A_0	A_1	A_2	A_3	A_4	σ
	313.15	−0.0246	−0.0258	0.0826	−0.1185	−0.0157	0.0001
	323.15	−0.0227	−0.0243	0.0900	−0.0176	−0.0207	0.0001
	333.15	−0.0201	−0.0277	0.0804	−0.0130	−0.0043	0.0002
{[EMIM]$^+$[EtSO$_4$]$^-$ (x_1) + acetophenone (x_2)}							
V_m^E/cm^3 mol^{-1}	293.15	−6.429	2.560	12.560	−13.367	1.413	0.047
	303.15	−5.957	2.654	12.016	−17.958	7.353	0.048
	313.15	−5.445	2.573	11.513	−21.042	11.573	0.042
	323.15	−4.893	2.374	11.120	−24.136	15.689	0.052
	333.15	−4.267	2.165	10.760	−27.585	20.393	0.025
$\Delta\kappa_s$/TPa^{-1}	293.15	−88 483	22 626	230 019	−262 334	17 006	706
	303.15	−98 751	32 880	187 116	−262 214	61 755	583
	313.15	−109 962	47 012	173 265	−265 702	36 968	782
	323.15	−117 269	52 626	148 852	−246 001	41 707	941
	333.15	−88 483	22 626	230 019	−262 334	17 006	706
$\Delta\eta$/mPa s	293.15	−139.733	50.296	−22.440	200.521	−190.369	1.098
	303.15	−76.920	31.738	1.307	110.531	−131.677	0.030
	313.15	−44.822	26.386	−17.842	71.022	−60.353	0.348
	323.15	−27.050	10.696	−46.834	51.453	−0.645	0.340
	333.15	−16.167	1.901	−19.639	28.183	−6.702	0.279
Δn	293.15	−0.0188	0.0002	0.0055	−0.0102	0.0707	0.0000
	303.15	−0.0175	0.0000	0.0090	−0.0090	0.0694	0.0001
	313.15	−0.0166	−0.0014	0.0161	−0.0040	−0.0612	0.0000
	323.15	−0.0149	−0.0008	0.0178	−0.0032	0.0613	0.0000
	333.15	−0.0138	−0.0028	0.0166	0.0014	0.0676	0.0001

a Metrohm 702 SM Titrino Metter before the experiments, and was found to be ≤0.06% in the chemicals used (Table 2).

2.2. Methods and procedure

The binary mixtures were prepared by transferring *via* syringe the pure liquids into stoppered bottles to prevent evaporation. The components were filled directly into the air-tight Stoppard 10 cm^3 glass vial and then weighed. For the determination of mass of each component, Radwag analytical mass balance was used with a precision of ±0.0001 g. The mixtures were shaken in order to ensure complete homogeneity of the compounds. After mixing the sample, the bubble-free homogeneous samples were injected into the vibration tube or sample cell of the densitometer, sound velocity analyzer, viscometer and refractor meter slowly using a medical syringe to avoid formation of bubbles inside the vibration tubes or sample cell. The chemicals were used without any further purification.

2.3. Density and sound velocity measurements

Density and sound velocity for various ILs, acetophenone and mixture of ILs with acetophenone were measured using a digital vibrating-tube densitometer and sound velocity analyzer (Anton Paar DSA 5000M) with an accuracy of ±0.02 K. The instrument measured simultaneously density in the range of (0 to 3) g cm^{-3} and sound velocity from (1000 to 2000) m s^{-1} in temperature range of (293.15 to 333.15) K with pressure variation from (0 to 0.3) MPa. The sound velocity was measured using a propagation time technique.[53] The samples were mediated between two piezoelectric ultrasound transducers. One transducer emits sound waves through the sample-filled cavity (frequency around 3 MHz) and the second transducer receives those waves.[67] Thus, the sound velocity was determined by dividing the known distance between transmitter and receiver by the measured propagation time of the sound waves.[53] The instrument was calibrated with dry air and freshly distilled degassed water once a day. The estimated error in density and speed of sound was less than ±2 × 10^{-4} g cm^{-3} and ±1 m s^{-1}, respectively. The estimated error in excess molar volume and deviation in isentropic compressibility was ±0.005 cm^3 mol^{-1} and ±1 TPa^{-1}, respectively.

2.4. Viscosity measurements

The viscosities measurements for pure components and their binary mixtures were determined using an Anton Paar Stabinger Viscometer (SVM 3000) fitted with jacketed small sample adapter (SSA) and a thermosel spindle (SC4-18) with an accuracy of ±0.02 K. Prior to each experimental run, the cell was firstly cleaned with deionised water (liquid 1) and then dried with acetone (liquid 2) using a fully automatic X-sample 452 Module which performed a cleaning routine after each measurement X-sample 452 performs a cleaning routine after each measurement. The estimated error in viscosity was less than ±0.05 mPa s. The instrument measured viscosity at temperature range of (293.15 to 333.15) K.

2.5. Refractive index measurements

Measurement of the refractive index for pure components and their binary mixtures were measured by a digital automatic

refractometer (Anton Paar RXA 156) with an accuracy of ±0.03 K. The estimated error in refractive index was less than ±0.005. The instrument measured refractive index at temperature range of (293.15 to 333.15) K.

2.6. Quantum chemical studies

In other to rationalize our experimental results, quantum chemical calculations were used to investigate the inter-ionic interactions between the cations and anions of the ionic liquids both in gaseous state and in continuum solvation with acetophenone by utilizing the integral formalism variant of the polarized continuum model (IEFPCM).[68]

Geometry optimizations of the molecular structures of $[BMIM]^+[BF_4]^-$, $[BMIM]^+[PF_6]^-$, $[EMIM]^+[BF_4]^-$ and $[EMIM]^+[EtSO_4]^-$ were done using the Density Functional Theory (DFT) method. The Perdew–Wang hybrid exchange–correlation functional (B3PW91)[69,70] and Pople-type split-valence triple-zeta basis set[71] augmented with diffuse and polarization functions on both the hydrogen and heavier atoms (6-311++G (d,p)) were selected for all the calculations. The B3PW91 (/6-311++G (d,p)) was selected because its adequate prediction of ionic liquids properties has been reported.[72–75] Frequency calculations were carried out on the optimized structures and the absence of imaginary frequencies confirmed that the optimized structures are true energy minima. Both geometry optimizations and frequency calculations were performed with ultrafine grid (99 radical and 590 angular points) to increase the accuracy of the results.[71] All the quantum chemical calculations were performed using Windows based Gaussian 09 suite version D.01.[76]

3. Results and discussion

3.1. Thermophysical and thermodynamics studies

In order to understand the influence of acetophenone on the thermophysical properties of the alkyl imidazolium-based ILs, the values of ρ, u, η and n_D for the binary mixtures of (ILs + acetophenone) systems were measured at temperature range (293.15 to 333.15) K under atmospheric pressure. Table 1 gives a clear indication that the studied ILs have higher ρ values than acetophenone at 303.15 K. The experimental values, ρ, u, η and n_D for the binary mixtures of alkyl imidazolium-based ionic liquids with acetophenone at temperature range (293.15 to 333.15) K as a function of IL concentration are presented in Table 1S (ESI†).

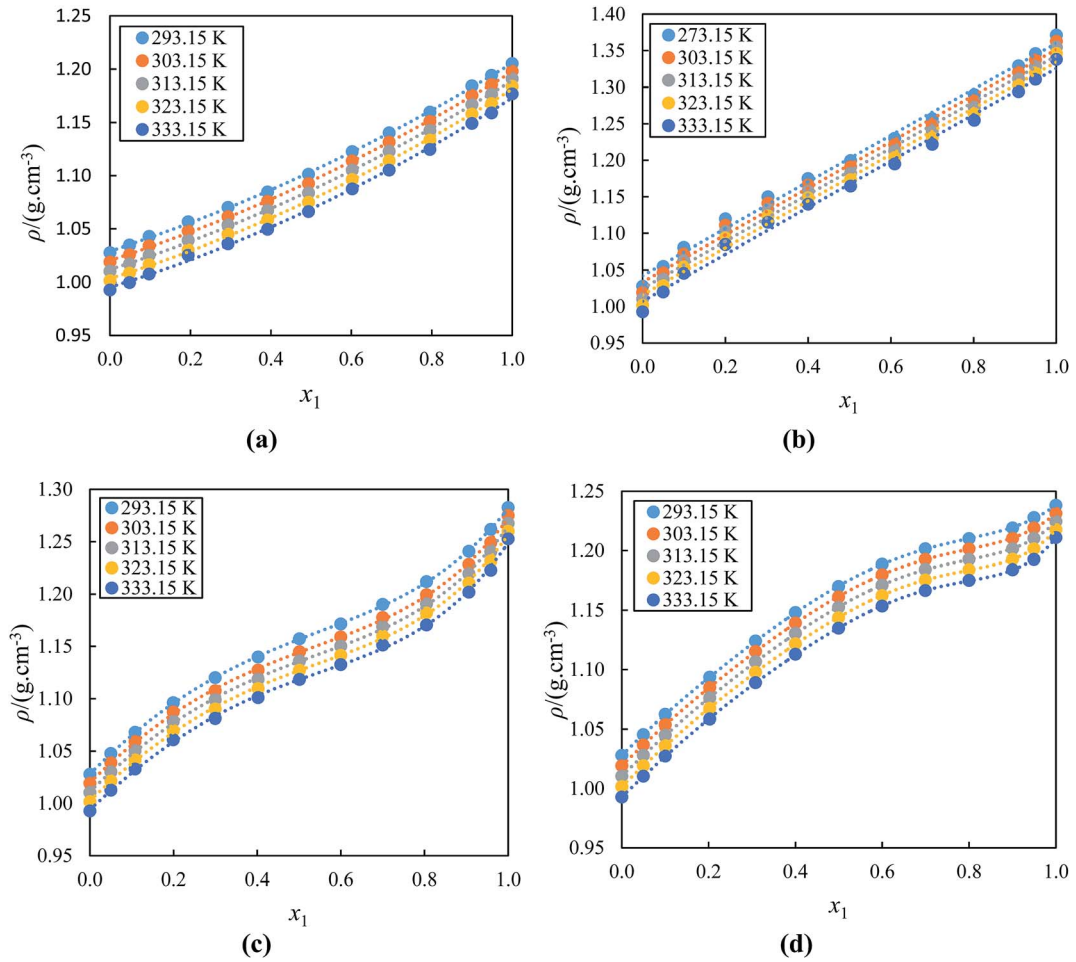

Fig. 1 Density (ρ) *vs.* mole fraction of IL for the mixtures of acetophenone with ILs (a) $[BMIM]^+[BF_4]^-$, (b) $[BMIM]^+[PF_6]^-$, (c) $[EMIM]^+[BF_4]^-$ and (d) $[EMIM]^+[EtSO_4]^-$ at (293.15, 303.15, 313.15, 323.15 and 333.15) K. The dotted line represents the smoothness of these data.

The values of ρ against the mole fraction of the IL at different temperature have been plotted in Fig. 1(a)–(d) for acetophenone and its binary mixtures with $[BMIM]^+[BF_4]^-$ or $[BIMIM]^+[PF_6]^-$ or $[EMIM]^+[BF_4]^-$ or $[EMIM]^+[EtSO_4]^-$, respectively. Results in Fig. 1(a)–(d) reveals that the ρ values for all studied binary mixtures increases as concentration of the IL in acetophenone increase and decreases with temperatures. In this study, ILs were completely miscible in acetophenone ($\varepsilon = 18.00$ at 298.15 K),[77] since acetophenone is a high dielectric liquid. The increase in the values of ρ for IL with acetophenone mixtures is as a result of an increase in the ion pair interactions between the IL and acetophenone. Increasing the temperature of the mixtures results in thermal agitation and causes molecules in the mixture to speed up and spread slightly further apart, occupying a larger volume hence decreasing the density. The thermophysical properties of ILs are dependent on the alkyl chain of the cation and nature of the structure of ions. The lower the alkyl chain length cation of the IL, the more dense compared to the higher alkyl chain length of the ILs, for example (1.20129 g cm^{-3} for $[BMIM]^+[BF_4]^-$ and 1.28174 g cm^{-3} for $[EMIM]^+[BF_4]^-$ at 293.15 K). This is mainly due to increase in dispersive interactions in ILs with increase in chain length, resulting in a nanostructured organization in polar and non-polar regions. The nonpolar regions are build-up of alkyl chains whereas the polar regions contain the cationic head groups and the anions. When the chain length of cation is enhanced, the nonpolar regions increase and take up more and more space, resulting in lower density in ILs with higher alkyl chain length.[78–80] Results obtained gives a proper indication that the ρ of the binary mixtures depend on the size of the cation and anion of the alkyl imidazolium-based ILs and the composition of the entire binary mixture. The ρ values at all temperatures of the alkyl imidazolium-based ILs with acetophenone follow the order: $[BMIM]^+[PF_6]^-$ > $[EMIM]^+[BF_4]^-$ > $[EMIM]^+[EtSO_4]^-$ > $[BMIM]^+[BF_4]^-$. This result show a clear indication of effect of cation and anion on ρ.[81] This order displays the highest ρ values due to the increased size of the anion with the same cation and *vice versa*.

The sound velocity of the (IL + acetophenone) mixtures presented in Fig. 2(a)–(d), shows that the size of the ions and the content of the acetophenone has an effect on the values of u for the studied binary mixtures. Practically, the u values of ILs mainly depend on the nature and structure of ions and the alkyl

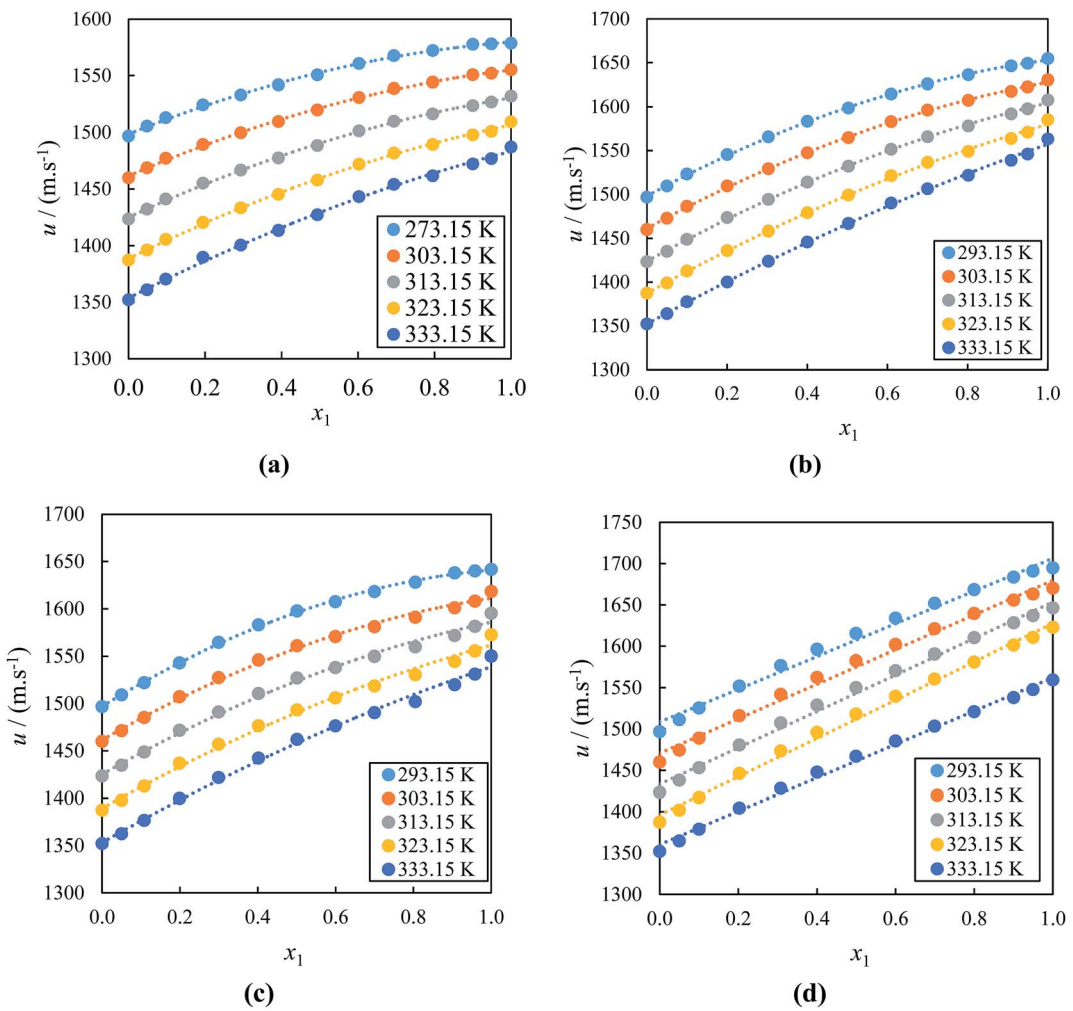

Fig. 2 Sound velocity (u) *vs.* mole fraction of IL for the mixtures of acetophenone with ILs (a) $[BMIM]^+[BF_4]^-$, (b) $[BMIM]^+[PF_6]^-$, (c) $[EMIM]^+[BF_4]^-$ and (d) $[EMIM]^+[EtSO_4]^-$ at (293.15, 303.15, 313.15, 323.15 and 333.15) K. The dotted line represents the smoothness of these data.

chain length of the cation. It can be clearly seen from Fig. 2(a)–(d) that at a given temperature, u values increased as the concentration of IL increased in the mixture and decreased as the temperature is increased for all studied systems. The u values at $T = 333.15$ K of the alkyl imidazolium-based ILs with acetophenone follow the order: $[BMIM]^+[PF_6]^-$ > $[EMIM]^+[EtSO_4]^-$ > $[EMIM]^+[BF_4]^-$ > $[BMIM]^+[BF_4]^-$. This order shows at the highest u values is due to the increased size of the anion. Further, the u values decrease as the cation alkyl chain length of ILs increases as seen in results with same anion. This is mainly due to anion accommodation closer to the cation. Apparently, ILs with higher cation side chain is accompanied by lower ρ and lower u. Therefore, our result demonstrates the influence of the cation and anion significantly affect the alkyl imidazolium-based ILs with acetophenone interactions. This may be also due to the stronger molecular interactions decreasing with increasing size of alkyl chain length of the cation of alkyl imidazolium-based ILs with acetophenone.[81]

With regard to the viscosity, the results displayed in Fig. 3(a)–(d) indicates that the values η for all studied binary mixtures increases as concentration of the IL in acetophenone increase due to the strong coulombic interactions between the ions of ILs. These are strengthened upon mixing with acetophenone, leading to lower mobility of ions which is partially based on smaller sizes of ions of ILs and also decreases with temperatures mainly due to increased Brownian motion of the constituent molecules of ILs.[81] It is clearly indicated that the (IL + acetophenone) mixtures are less viscous than pure ILs yet more viscous than acetophenone. In contrast to the ρ which increases with a decrease in the alkyl chain length of the cation, the values of η increases with an increase in alkyl side chain length of the cation if the system have a common anion. The η values for ($[BMIM]^+[BF_4]^-$ + acetophenone) binary mixture are higher compared to ($[EMIM]^+[BF_4]$ + acetophenone) binary mixture. This results from an increase in the van der Waals interactions between alkyl side chains of the cation and the proportion of the charged species in an entire mixture. It is clear

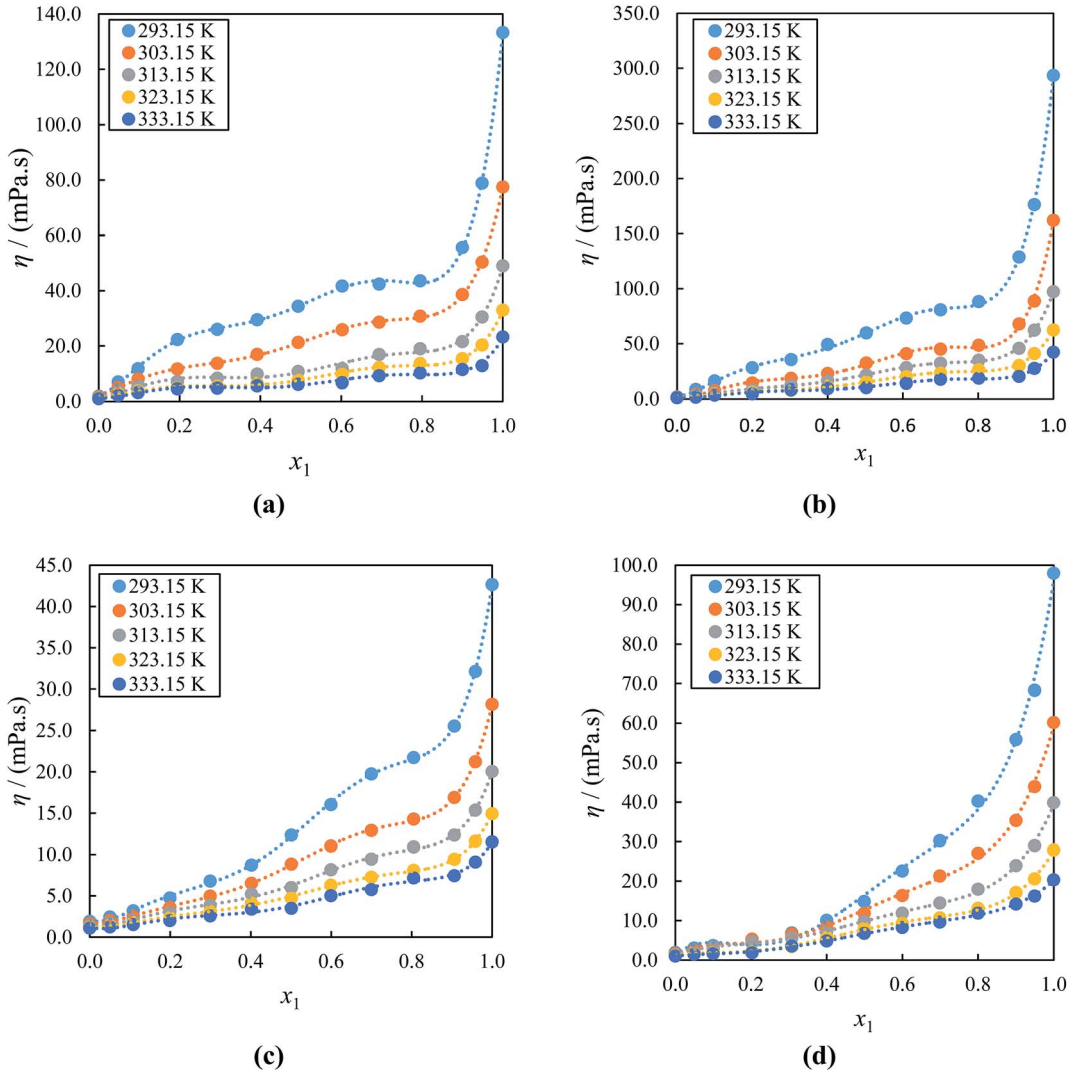

Fig. 3 Viscosity (η) *vs.* mole of IL for the mixtures of acetophenone with ILs (a) $[BMIM]^+[BF_4]^-$, (b) $[BMIM]^+[PF_6]^-$, (c) $[EMIM]^+[BF_4]^-$ and (d) $[EMIM]^+[EtSO_4]^-$ at (293.15, 303.15, 313.15, 323.15 and 333.15) K. The dotted line represents the smoothness of these data.

that these results possibly imply that the cation size has an effect on the variation of the thermophysical properties of ILs in mixture with acetophenone. Furthermore, it can be seen that η values for ($[EMIM]^+[EtSO_4]^-$ + acetophenone) binary mixture are higher compared to ($[EMIM]^+[BF_4]$ + acetophenone) binary mixture. This is mainly due to the nature of the anion which also affects the η of ILs with same cation, particularly through relative basicity and the ability to form the hydrogen bonding. The η values at all temperatures of the alkyl imidazolium-based ILs with acetophenone follow the order: $[BMIM]^+[PF_6]^-$ > $[BMIM]^+[BF_4]^-$ > $[EMIM]^+[EtSO_4]^-$ > $[EMIM]^+[BF_4]^-$ with may be due to the increased alkyl chain of the cation.

Fig. 4(a)–(d) shows the measured values of n_D for alkyl imidazolium-based ILs with acetophenone at (293.15, 303.15, 313.15, 323.15 and 333.15) K over the entire composition range plotted against the mole fraction of the IL. The values of n_D decreased with increasing concentration and temperature of IL in the mixture due to the ion–ion pair interactions between the IL and acetophenone The n_D values at T = 293.15 K of the alkyl imidazolium-based ILs with acetophenone follow the order: $[EMIM]^+[EtSO_4]^-$ > $[BMIM]^+[BF_4]^-$ > $[EMIM]^+[BF_4]^-$ ≈ $[BMIM]^+[PF_6]^-$. This order clearly shows that $[EtSO_4]^-$ anion has higher n_D values with same cation $[EMIM]^+$ IL as compared to $[BF_4]^-$ anion due to the ions arrangement and an efficient packing of ions of ILs.[77] This result also indicated that the alkyl chain of cation decreases as n_D values increases with the same anion but different cation. There are no previous, ρ, u, η and n_D data reported in the literature for studied systems at various temperatures for comparison.

The obtained experimental thermo-physical properties; ρ, u, η and n_D of the alkyl imidazolium-based ILs and their mixtures with acetophenone were further used to obtain the derived thermodynamics properties; V_m^E, $\Delta\kappa_s$, $\Delta\eta$ and Δn using the standard equations in order to give an excellent estimation of the strength of unlike molecular interactions in the solution. These properties were fitted to the Redlich–Kister[82] polynomial equation to check the accuracy of experimental results.

$$X = x_1 x_2 \sum_{i=1}^{k} A_i (1 - 2x_1)^{i-1} \quad (1)$$

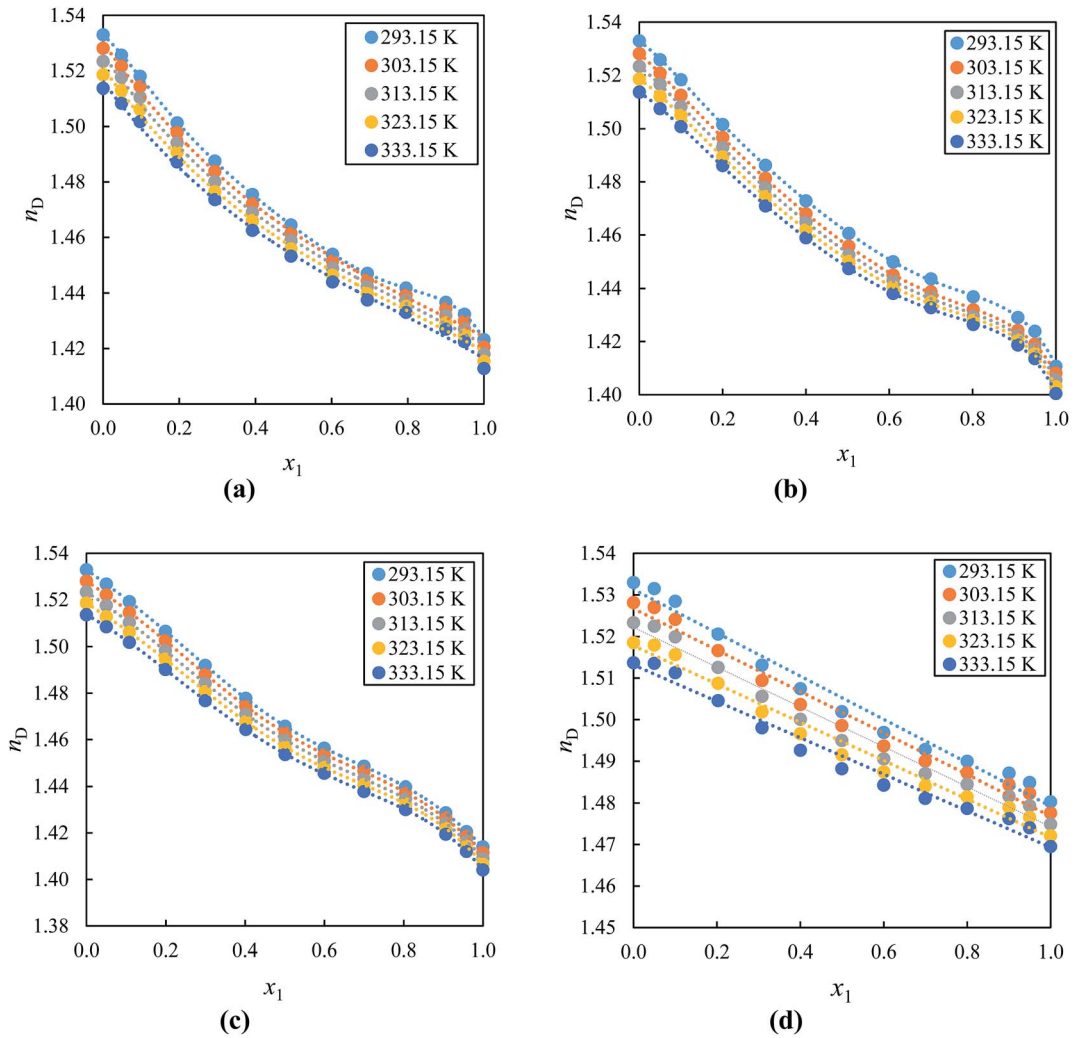

Fig. 4 Refractive index (n_D) *vs.* mole fraction of IL for the mixtures of acetophenone with ILs (a) $[BMIM]^+[BF_4]^-$, (b) $[BMIM]^+[PF_6]^-$, (c) $[EMIM]^+[BF_4]^-$ and (d) $[EMIM]^+[EtSO_4]^-$ at (293.15, 303.15, 313.15, 323.15 and 333.15) K. The dotted line represents the smoothness of these data.

Table 3 Interaction energies and change in Gibbs free energies of ionic liquid systems in gaseous state and solvent

	Gaseous state		Acetophenone	
ILs	ΔE_{int} (kJ mol^{-1})	ΔG (kJ mol^{-1})	ΔE_{int} (kJ mol^{-1})	ΔG (kJ mol^{-1})
$[BMIM]^+[BF_4]^-$	−337.79	−294.80	−22.04	11.93
$[BMIM]^+[PF_6]^-$	−310.62	−273.16	−14.05	13.01
$[EMIM]^+[BF_4]^-$	−338.10	−297.64	−25.91	4.27
$[EMIM]^+[EtSO_4]^-$	−350.71	−302.36	−24.92	11.44

$$\sigma(X) = \sum_{i=1}^{N} \left[\frac{(X_{expt} - X_{calc})^2}{(N-k)} \right]^{1/2} \quad (2)$$

where N is the number of experimental data point, X refers to V_m^E, $\Delta\kappa_s$, $\Delta\eta$ and Δn; x_1 and x_2 are mole fractions of pure compounds 1 and 2. The values of the fitting parameters A_i have been determined using a least-square method. These results are summarized in Table 3, together with the corresponding standard deviations, σ, for the correlation as determined using the eqn (2).

The obtained values of V_m^E, $\Delta\kappa_s$, $\Delta\eta$ and Δn for the binary mixtures of alkyl imidazolium-based ILs with acetophenone at (293.15 to 333.15) K as a function of IL concentration are also presented in Table 1S.† Fig. 5(a) and (b) which are the V_m^E graphs of ILs with acetophenone, depicts positive values over the entire mole fraction range at (293.15 to 333.15) K for binary systems ($[BMIM]^+[PF_6]^-$ or $[BMIM]^+[BF_4]^-$ + acetophenone), while both positive and negative values for the systems ($[EMIM]^+[BF_4]^-$ or $[EMIM]^+[EtSO_4]^-$ + acetophenone) with negative values up to $x_1 \approx 0.3000$, and ≈ 0.8000 and positive values over the remaining

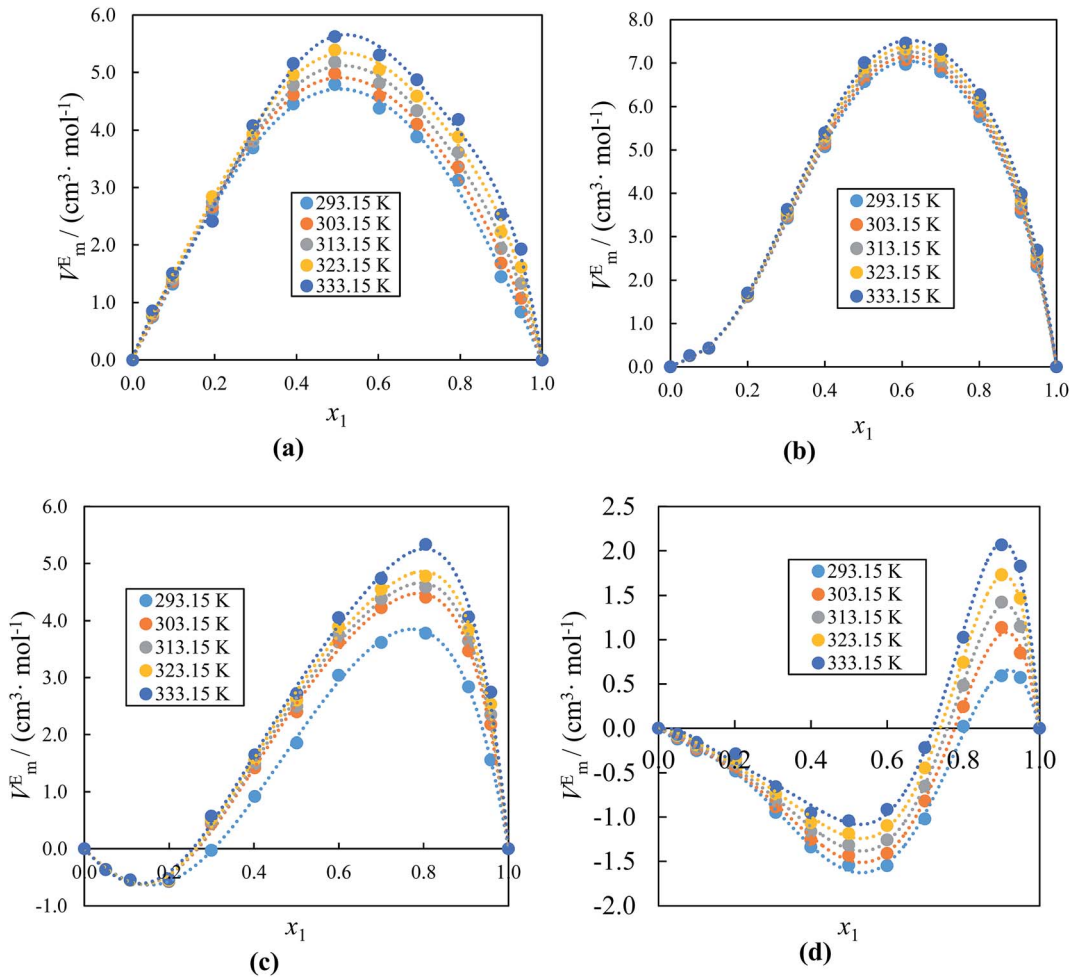

Fig. 5 Excess molar volume (V_m^E) *vs.* mole fraction of IL for the mixtures of acetophenone with ILs (a) $[BMIM]^+[BF_4]^-$, (b) $[BMIM]^+[PF_6]^-$, (c) $[EMIM]^+[BF_4]^-$ and (d) $[EMIM]^+[EtSO_4]^-$ at (293.15, 303.15, 313.15, 323.15 and 333.15) K. The dotted lines were generated using Redlich–Kister curve-fitting.

mole fraction indicated in Fig. 5(c) and (d), respectively. As the mole fraction of IL increases the negative V_m^E increases sharply up to $x_1 \approx 0.2000$, and 0.6000, while with further addition of the ILs there is a decrease in the excess molar volume graph at all temperature ranges as seen in Fig. 5(c) and (d). This may reveal that more efficient packing is due to the differences in size and shape of molecules in the mixtures or attractive interaction occurs in the region of low mole fraction of IL. Furthermore, the negative V_m^E values of acetophenone-rich region of ($[EMIM]^+[BF_4]^-$ or $[EMIM]^+[EtSO_4]^-$ + acetophenone) becomes positive V_m^E values at higher IL concentration region. This inconsistency may be due to the variation from IL to IL (depending on the cation/anion size) as well as solvent to solvent and also depend on the nature of the structural arrangement of ILs and acetophenone. The positive values shows that there is a volume expansion mixing of IL. There is less volume contraction due to the interactions between unlike molecules which are weaker. The negative values shows that more attractive interactions in the mixtures than in the pure components and the systems have a strong packing effect by associations between ILs and acetophenone molecules through hydrogen bonding. The dependency of V_m^E on temperature and composition for the mixture can be described as the difference in intermolecular forces between the compounds or the variation in the molecular packing, which results from the differences in size and shape of the molecules forming a binary mixture with other compounds.[83] The results in Fig. 5 show that the V_m^E values increase with increasing temperature for all systems at a fixed composition, indicating the deviation from ideal behavior to become pronounced as the temperature is increased. These observations can be attributed to the natural complexity of the IL with acetophenone systems as far as interactions with in the system are concerned. From Fig. 5, it can be noted that the magnitude of V_m^E values for ILs with acetophenone at studied temperature follow the order: $[BMIM]^+[PF_6]^-$ > $[BMIM]^+[BF_4]^-$ > $[EMIM]^+[BF_4]^-$ > $[EMIM]^+[EtSO_4]^-$. From this order, it can be seen that the increase of the alkyl chain length of cation on the IL from $[BMIM]^+$ to $[EMIM]^+$ strongly affect the V_m^E values of the solutions. At T = 333.15 K, the positive V_m^E values for ($[BMIM]^+[BF_4]^-$ + acetophenone) (V_m^E = 5.623 cm^3 mol^{-1} at

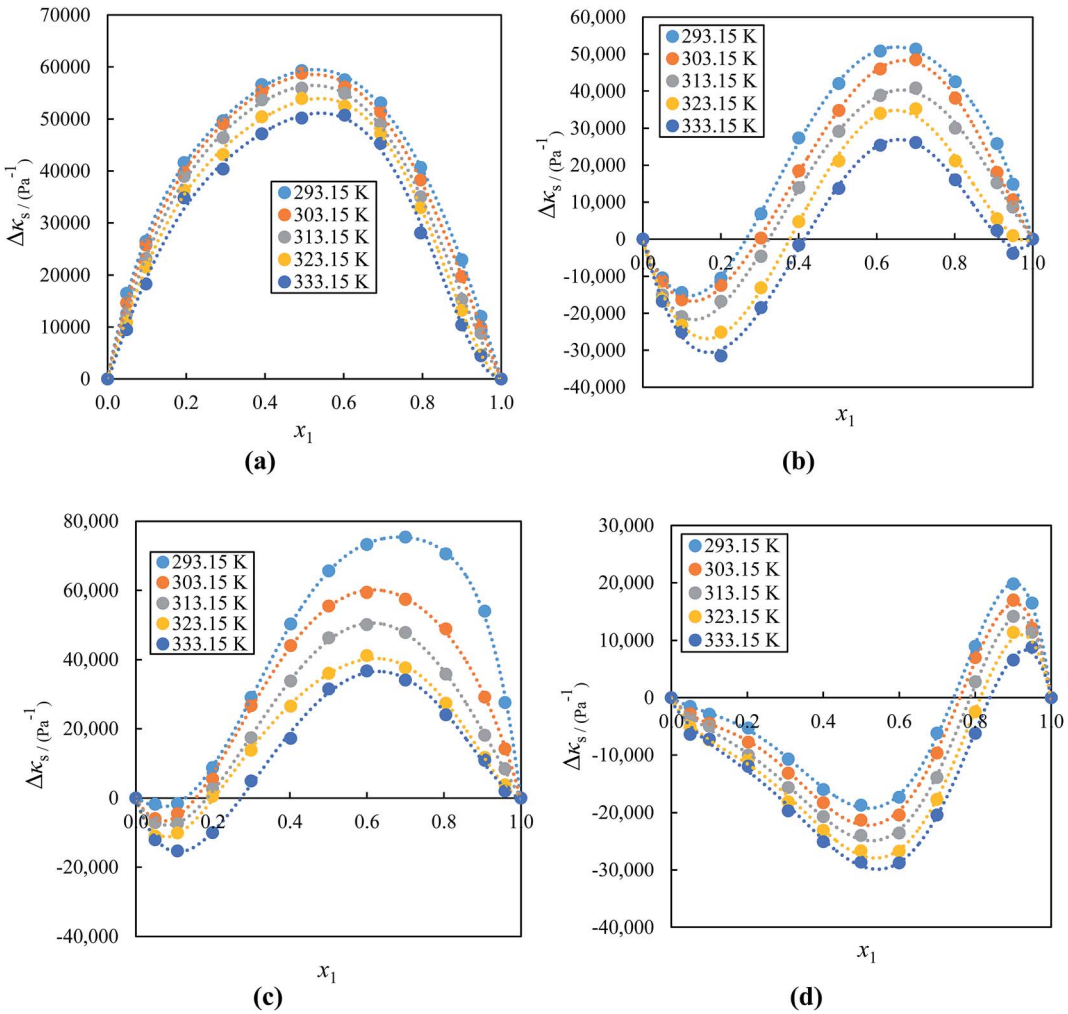

Fig. 6 Deviation in isentropic compressibility ($\Delta\kappa_s$) *vs.* mole fraction of IL for the mixtures of acetophenone with ILs (a) $[BMIM]^+[BF_4]^-$, (b) $[BMIM]^+[PF_6]^-$, (c) $[EMIM]^+[BF_4]^-$ and (d) $[EMIM]^+[EtSO_4]^-$ at (293.15, 303.15, 313.15, 323.15 and 333.15) K. The dotted lines were generated using Redlich–Kister curve-fitting.

x_1 = 0.4936) are more positive than for the system ([EMIM]$^+$[BF_4]$^-$ + acetophenone) (V_m^E = 2.721 cm^3 mol^{-1} x_1 = 0.5011) while having the same anion [BF_4]$^-$, therefore V_m^E values become more positive in higher alkyl length of the IL cation under the same experimental condition. The more positive V_m^E values for ([BMIM]$^+$[PF_6]$^-$ + acetophenone) serves as an evidence that higher alkyl chain molecules decrease the hydrogen bonding tendency between [BMIM]$^+$ with acetophenone. On the other hand, the ([EMIM]$^+$[$EtSO_4$]$^-$ + acetophenone) mixture reveals less positive values of V_m^E than other studied systems, which imply that [EMIM]$^+$[$EtSO_4$]$^-$ ion–dipole interactions and packing effects with acetophenone are stronger than those in the other systems. Clearly, it is also shown that the nature of interactions in ILs with acetophenone systems is highly dependent on nature of the ions as well as anion. It is quite clear from Fig. 5 that anion structure in alkyl imidazolium-based ILs strongly affects the V_m^E values. It was found that [PF_6]$^-$ anion exhibit more positive V_m^E values than the corresponding [BF_4]$^-$ anion with same cation [BMIM]$^+$ and also [BF_4]$^-$ anion more than [$EtSO_4$]$^-$ anion with same cation [EMIM]$^+$. It has been shown that the values of V_m^E also depend on the basicity as well as size of the anion.

Fig. 6(a)–(d) shows the graphs for $\Delta\kappa_s$ against the mole fraction at (293.15 to 333.15) K. As seen in Fig. 6(a), the values for $\Delta\kappa_s$ are all positive for the whole compositions for the system ([BMIM]$^+$[BF_4] + acetophenone) and both positive and negative for the systems ([BMIM]$^+$[PF_6] or [EMIM]$^+$[BF_4]$^-$ or [EMIM]$^+$[$EtSO_4$]$^-$ + acetophenone) negative up to $x_1 \approx 0.3000$, $\approx$0.4000 and $\approx$0.8000 and positive over the remaining mole fraction indicated in Fig. 6(b)–(d), respectively at all temperatures. The negative $\Delta\kappa_s$ values are attributed to the strong attractive interactions of the ions in the mixture due to the solvation of the ions in the acetophenone. The negative values of the $\Delta\kappa_s$ of an alkyl imidazolium-based ILs with acetophenone implies that acetophenone molecules around the ILs are less compressible than the solvent molecules in the bulk solutions. As the mole fraction of IL increases, the negative deviation increases sharply up to $x_1 \approx 0.1000$, 0.0500, and 0.5000, while

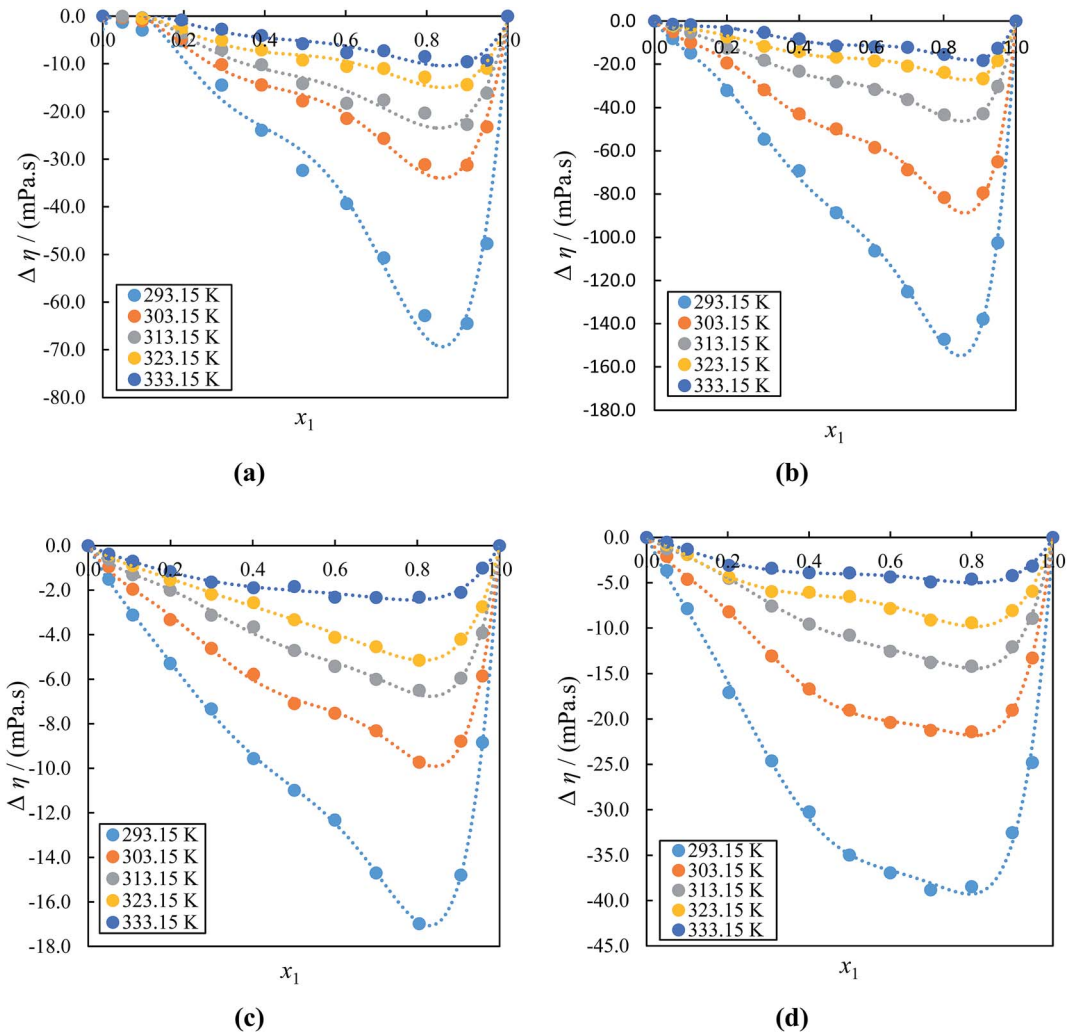

Fig. 7 Deviation in viscosity (Δη) *vs.* mole fraction of IL for the mixtures of acetophenone with ILs (a) [BMIM]$^+$[BF_4]$^-$, (b) [BMIM]$^+$[PF_6]$^-$, (c) [EMIM]$^+$[BF_4]$^-$ and (d) [EMIM]$^+$[$EtSO_4$]$^-$ at (293.15, 303.15, 313.15, 323.15 and 333.15) K. The dotted lines were generated using Redlich–Kister curve-fitting.

with further addition of the ILs there is a decrease in the compressibility graph at all temperature ranges. This might be due to a decrease in attraction of acetophenone and IL molecules in the IL-rich concentration region, since the interaction between the IL to IL increases and that between IL to acetophenone decreases. On the other hand, the negative $\Delta\kappa_s$ values of acetophenone-rich region of ($[BMIM]^+[PF_6]$ or $[EMIM]^+[BF_4]^-$ or $[EMIM]^+[EtSO_4]^-$ + acetophenone) becomes positive $\Delta\kappa_s$ values at higher IL concentration region. These inconsistencies vary from IL to IL (depending on the cation/anion size) and solvent to solvent as well as also depend on the nature of the structural arrangement of IL and solvent. The positive values of $\Delta\kappa_s$ for binary mixtures of IL with acetophenone are possibly attributed to the repulsive forces due to the electric charge of components and therefore, the molecular interactions between IL and acetophenone molecules weaken. The results in Fig. 6 show that the $\Delta\kappa_s$ values decrease with increasing temperature for all systems at a fixed composition. These results are in good agreement with those obtained from the volumetric studies. On the other hand, the values followed the order $[EMIM]^+[EtSO_4]^-$ > $[EMIM]^+[BF_4]^-$ > $[BMIM]^+[BF_4]^-$ > $[BMIM]^+[PF_6]^-$. The $\Delta\kappa_s$ values decreases as alkyl chain length of cation increases and have higher values for $[EMIM]^+[EtSO_4]^-$. These results reveal that $\Delta\kappa_s$ values also depend on size of anion with the same cation.

Fig. 7(a)–(d) which shown the $\Delta\eta$ graphs of ILs with acetophenone, reveals that the values are all negative and become less negative with increasing temperature over a wide mole fraction range at (293.15 to 333.15) K under atmospheric pressure, and the minimum existed at IL region; *i.e.*, $x_1 \approx 0.8000$–0.9000 and these curves are asymmetric. The minimum $\Delta\eta$ values are −64.48 mPa s (at $x_1 \approx 0.8999$), −147.27 mPa s (at $x_1 \approx 0.8017$), −16.98 mPa s (at $x_1 \approx 0.8050$) and −38.83 mPa s (at $x_1 \approx 0.6992$) for ($[BMIM]^+[BF_4]^-$ or $[BMIM]^+[PF_6]$ or $[EMIM]^+[BF_4]^-$ or $[EMIM]^+[EtSO_4]^-$ + acetophenone) systems, respectively. The negative $\Delta\eta$ values may be attributed to the formation of weak hydrogen bonding interactions between the ions of ILs with acetophenone. These results clearly show that the $\Delta\eta$ data is more affected with anions of alkyl imidazolium cation of ILs, which indicates that the interactions become weak between the ions of ($[BMIM]^+[PF_6]$ + acetophenone) than

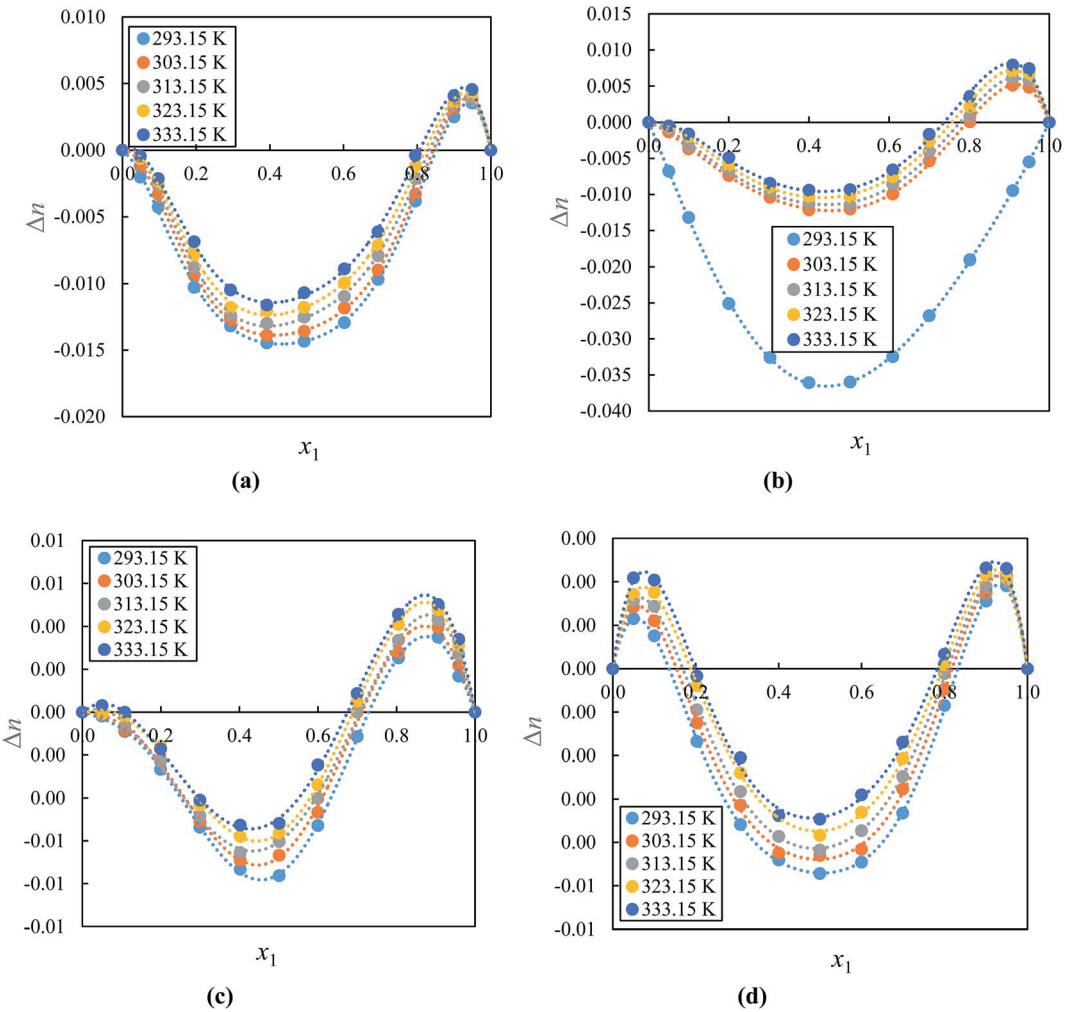

Fig. 8 Deviation in refractive index (Δn_D) *vs.* mole fraction of IL for the mixtures of acetophenone with ILs (a) $[BMIM]^+[BF_4]^-$, (b) $[BMIM]^+[PF_6]^-$, (c) $[EMIM]^+[BF_4]^-$ and (d) $[EMIM]^+[EtSO_4]^-$ at (293.15, 303.15, 313.15, 323.15 and 333.15) K. The dotted lines were generated using Redlich–Kister curve-fitting.

($[BMIM]^+[BF_4]^-$ + acetophenone) and ($[EMIM]^+[EtSO_4]^-$ + acetophenone) than ($[EMIM]^+[BF_4]^-$ + acetophenone) systems due to weakening of the dipolar association by ILs. The negative $\Delta\eta$ values of $[BMIM]^+$ cation with same anion is higher than $[EMIM]^+$ cation due to the steric hindrance of alkyl chain groups in $[BMIM]^+$ cations. When acetophenone is added to the IL, the viscosities of the mixtures decreases faster, mainly at lower temperatures. The strong coulomb interaction between the anions and cations becomes upon adding acetophenone, which in turn leads to a higher mobility of the ions and hence a lower viscosity of the mixtures.[83] Therefore the values of $\Delta\eta$ are negative in all cases.

The "Δn_D" values can be used to determine of the electronic polarizability of a molecule and provide useful information about the intermolecular interactions between molecules. However, an accurate Δn_D data for ILs with molecular solvents are still scarce. Fig. 8(a)–(d) show Δn_D for binary mixture of alkyl imidazolium-based ILs with acetophenone and indicates that both negative and positive values for Δn_D over a wide mole fraction range at (293.15 to 333.15) K under atmospheric pressure show curves that are asymmetric with minimum and maximum reaching near to 0.4000–0.6000 and 0.9000 mole fraction of IL, respectively. The Δn_D values increases as temperature increased. The positive values of Δn_D may be due to the stronger interactions of ions of ILs with acetophenone and negative values attributed to weaker interaction ions of ILs with acetophenone. The values for Δn_D are dependent mainly on the difference in intermolecular interactions occurring between the two components. It can be seen that positive or negative V_m^E values corresponded to negative or positive Δn_D values; the minimum or maximum of both values exist at almost the same mole fraction of IL of corresponding systems. On the other hand, the values followed the order: $[EMIM]^+[BF_4]^-$ > $[EMIM]^+[EtSO_4]^-$ > $[BMIM]^+[PF_6]^-$ > $[BMIM]^+[BF_4]^-$. These results reveal that Δn_D values also depend on size of anion with the same cation. The opposite signs between V_m^E and Δn_D can be attributed to less free volume available (if V_m^E is negative) and more free volume available (if V_m^E is positive) than in an ideal solution and photons will be more likely to interact with molecules or ions constituting the compound.[84–87] These results are in good agreement with those obtained from the volumetric and acoustic studies.

3.2. Quantum chemical studies

Quantum chemical calculations have been employed complement our experimental findings on the interactions existing

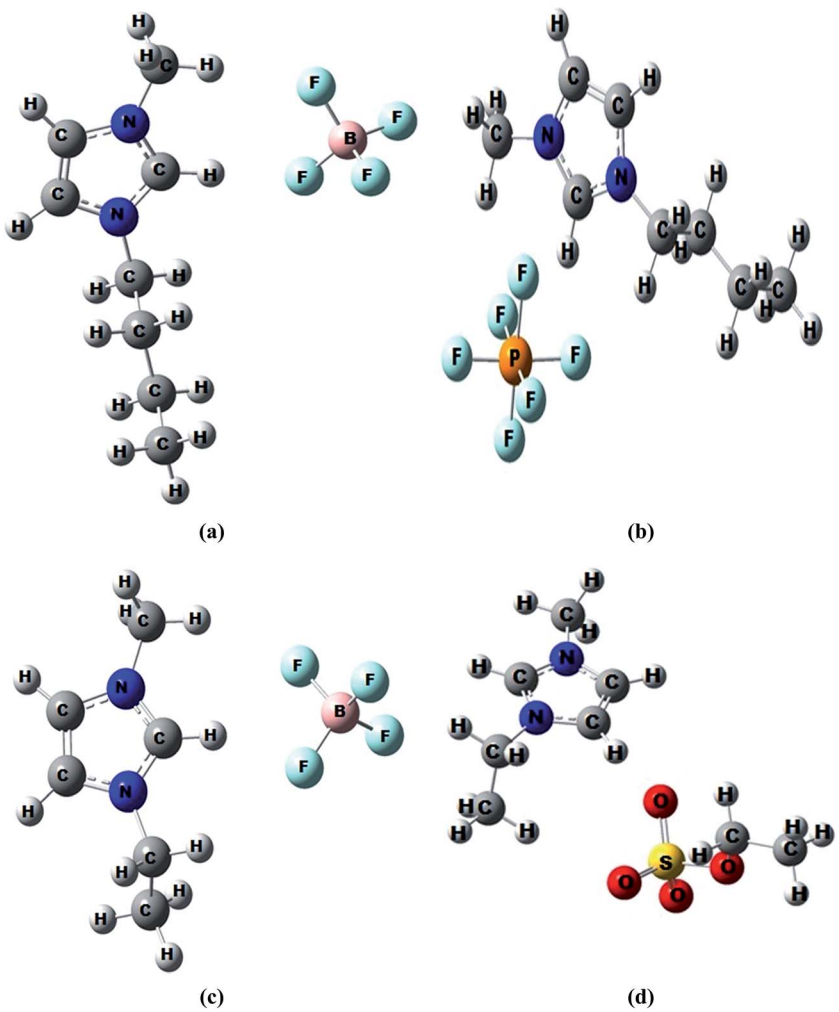

Fig. 9 Optimized structures of ionic liquids (a) $[BMIM]^+[BF_4]^-$, (b) $[BMIM]^+[PF_6]^-$, (c) $[EMIM]^+[BF_4]^-$, (d) $[EMIM]^+[EtSO_4]^-$.

between the ionic liquids studied and acetophenone. Isolated structures of the anions ($[PF_6]^-$, $[BF_4]^-$ and $[EtSO_4]^-$) and cations ($[BMIM]^+$ and $[EMIM]^+$) as well as molecular structures of the ionic liquids were optimized. Optimized structures of ionic systems are shown in Fig. 9. The interaction energies (ΔE_{int}) for the ionic liquid systems were calculated from the stabilization energy difference according to eqn (3):

$$\Delta E_{int} = E(ac) - (E(a) + E(c)) \quad (3)$$

where E(a) and E(c) are the energies of the pure anion and cation, respectively, and E(ac) the energy of ionic liquid system. All calculated energies are corrected by zero point energy (ZPE), using an empirical scaling factor of 0.972.[88]

Frequency calculations were also done on the optimized structures from which the change in Gibb's free energy (ΔG) for the cation–anion interaction was calculated. The interaction energies and change in Gibb's free energies are given in Table 3.

More negative ΔE_{int} is an indication of stronger interaction when comparing interactions between two or more systems.[89,90] As shown in the Table 3, ΔE_{int} of the ionic systems in the presence of acetophenone remarkably increased (less negative) as compared to when they were without the solvent. This is an indication of appreciable decrease in the cation–anion interaction in the presence of the solvent.[91] This can be attributed to the separate interactions of the cations and anions of the ionic liquids with the acetophenone molecules (*i.e.* ion–solvent interactions) rather than with each other (*i.e.* cation–anion interactions).[69,90] The ion–solvent interaction reduces the cation–anion interaction by reducing the number of anion–cation pairs that are available for the cation–anion interaction.[91,92]

The ΔE_{int} of the studied ionic liquid in solvent system, followed the order $[BMIM]^+[PF_6]^-$ > $[BMIM]^+[BF_4]^-$ > $[EMIM]^+[EtSO_4]^-$ > $[EMIM]^+[BF_4]^-$. This trend shows that the extent of the solvent–ion interactions in ionic liquids follows the same order because the lower the cation–anion interaction (*i.e.* less negative ΔE_{int}), the greater the ion–solvent interaction. The change in Gibb's free energy (ΔG) of the ionic systems also follows the similar trend as ΔE_{int} indicates a reduced spontaneity of the cation–anion interactions in the presence of the acetophenone in the order $[BMIM]^+[PF_6]^-$ > $[BMIM]^+[BF_4]^-$ > $[EMIM]^+[EtSO_4]^-$ > $[EMIM]^+[BF_4]^-$ because of energetically more favourable solvent–ion interaction. The $[BMIM]^+[PF_6]^-$ system has the highest ΔG (13.01 kJ mol^{-1}) which means the cation–anion interaction is least favourable and automatically the solvent–ion interaction is most favourable in this system relative to other systems of study.

4. Conclusions

This study report on new data for densities (ρ), sound velocities (u), viscosities (η), and refractive indices (n_D) of binary mixtures of four alkyl imidazolium-based ionic liquids which have same anion and different anion and *vice versa*; $[BMIM]^+[BF_4]^-$, $[BMIM]^+[PF_6]^-$, $[EMIM]^+[BF_4]^-$ and $[EMIM]^+[EtSO_4]^-$, with acetophenone over the wide composition range at (293.15 to 333.15) K under atmospheric pressure. The study illustrated the effect of temperature, concentration as well as cation/anion of ILs on the molecular interaction behavior of alkyl imidazolium-based IL with acetophenone. From experimental data, excess and derived properties such as V_m^E, $\Delta\kappa_s$, $\Delta\eta$ and Δn_D were calculated and fitted to Redlich–Kister equation to check the accuracy of experimental results and found to be in good agreement with experimental results. Our results reveal that the values of, ρ, u and η increases as concentration of the IL increases whereas opposite trend was observed for n_D and all the other measured properties decreases with temperatures. Results obtained indicates that the ρ, u and Δn_D values decrease with increase in the cation alkyl chain length, however an opposite trend was observed, in which the values of η increase when the number of carbon atoms in the alkyl chain length of cation of ILs increases. The experimental data indicate that cation and anion of ILs have a strong influence on the excess and deviation properties, especially on excess molar volume. Quantum chemical studies confirm the interactions of acetophenone with the ILs and also show that the solvent–ion interaction is highest in $[BMIM]^+[PF_6]^-$ system and lowest in $[EMIM]^+[BF_4]^-$ thereby confirming the experimental results.

Acknowledgements

The authors acknowledge funding from North-West University, Department of Science and Technology and the National Research Foundation (DST/NRF) South Africa for M. Kgomotso and Dr I. Bahadur, respectively.

References

1 P. Sun and D. W. Armstrong, *Anal. Chim. Acta*, 2010, **661**, 1–16.
2 K. N. Marsh, J. A. Boxall and R. Lichtenthaler, *Phys. Chem. Chem. Phys.*, 2004, **219**, 93–98.
3 M. Freemantle, *An introduction to ionic liquids*, Royal Society of Chemistry, Cambridge, 2010, ch. 1, pp. 1–10.
4 Z. Yang and W. Pan, *Enzyme Microb. Technol.*, 2005, **37**, 19–28.
5 V. H. Alvarez, S. Mattedi, M. Martin-Pastor, M. Aznar and M. Iglesias, *J. Chem. Thermodyn.*, 2011, **43**, 997–1010.
6 A. E. Andreatta, A. Arce, E. Rodil and A. Soto, *J. Chem. Eng. Data*, 2009, **54**, 1022–1028.
7 S. Keskin, D. Kayrak-Talay, U. Akman and O. Hortac, *J. Supercrit. Fluids*, 2007, **43**, 150–180.
8 G. Laus, G. Bentivoglio, H. Schottenberger, V. Kahlenberg, H. Kopacka, T. Röder and H. Sixta, *Lenzinger Ber.*, 2005, **84**, 71–85.
9 Y. Xu, J. Yao, C. Wang and H. Li, *J. Chem. Eng. Data*, 2012, **57**, 298–308.
10 D. Han and K. H. Row, *Molecules*, 2010, **15**, 2405–2426.
11 D. Shao, X. Lu, W. Fang, Y. Guo and L. Xu, *J. Chem. Eng. Data*, 2012, **57**, 937–942.
12 H. Yao, S. Zhang, J. Wang, Q. Zhou, H. Dong and X. Zhang, *J. Chem. Eng. Data*, 2012, **57**, 875–881.
13 Y. Zhong, H. Wang and K. Diao, *J. Chem. Thermodyn.*, 2007, **39**, 291–296.

14 V. V. Singh, K. Nigam, A. Batra, M. Boopathi, B. Singh and R. Vijayaraghavan, *Int. J. Electrochem.*, 2012, **2012**, 1–19.
15 M. Almasi and H. Iloukhani, *J. Chem. Eng. Data*, 2010, **55**, 1416–1420.
16 M. N. Roy, B. K. Sarkar and R. Chanda, *J. Chem. Eng. Data*, 2007, **52**, 1630–1637.
17 M. Sittig, *Handbook of Toxic and Hazardous Chemicals and Carcinogens*, Noyes Publications, Park Ridge, NJ, 2nd edn, 1985.
18 J. M. Prausnitz, *Fluid Phase Equilib.*, 1999, **95**, 158–160.
19 P. B. Mandal, K. Madhusree and S. S Bandyopadhyay, *J. Chem. Eng. Data*, 2003, **48**, 703–707.
20 M. J. Dávila, S. Aparicio and R. Alcalde, *Ind. Eng. Chem. Res.*, 2009, **48**, 10065–10076.
21 Y. Maham, L. Lebrette and A. E. Mather, *J. Chem. Eng. Data*, 2002, **47**, 550–553.
22 P. Abrman and I. Malijevská, *Fluid Phase Equilib.*, 1999, **166**, 47–52.
23 Z. Zhou, Y. Shi and X. Zhou, *J. Phys. Chem. A*, 2004, **108**, 813–822.
24 W. Dongqing, J. F. Truchon, S. Sirois and D. Salahub, *J. Chem. Phys.*, 2002, **116**, 6028–6038.
25 G. F. Velardez, J. C. Ferrero, J. A. Beswick and J. A. Dudey, *J. Phys. Chem. A*, 2001, **105**, 8769–8774.
26 S. Zhang, N. Sun, X. He, X. Lu and X. Zhang, *J. Phys. Chem.*, 2006, **35**, 1475–1517.
27 B. González, N. Calvar, E. González and A. Domínguez, *J. Chem. Eng. Data*, 2008, **53**, 881–887.
28 A. B. Pereiro, J. L. Legido and A. Rodríguez, *J. Chem. Thermodyn.*, 2007, **39**, 1168–1175.
29 G. Annat, M. Forsyth and D. R. MacFarlane, *J. Phys. Chem. B*, 2012, **116**, 8251–8258.
30 M. Deetlefs, K. R. Seddon and M. Shara, *Phys. Chem. Chem. Phys.*, 2006, **8**, 642–649.
31 A. Kovács, R. J. M. Konings, J. K. Gibson, I. Infante and L. Gagliardi, *Chem. Rev.*, 2015, **115**, 1725–1759.
32 A. Jardy, A. L. Lasalle-Molin, M. Keddam and H. Takenouti, *Electrochim. Acta*, 1993, **37**, 2195–2201.
33 D. Tromans, *J. Electrochem. Soc.*, 1998, **145**, L42–L45.
34 R. Walter, *Corrosion*, 1973, **29**, 290–298.
35 V. Brusic, M. A. Frisch, B. N. Eldridge, F. P. Novak, F. B. Kaufman, B. M. Rush and G. S. Frankel, *J. Electrochem. Soc.*, 1991, **138**, 2253–2259.
36 S. L. F. da Costa, S. M. L. Agostinho and K. Nobe, *J. Electrochem. Soc.*, 1993, **140**, 3483–3488.
37 D. Tromans and R. Sun, *J. Electrochem. Soc.*, 1991, **138**, 3235–3244.
38 T. E. Shubina and M. T. M. Koper, *Electrochim. Acta*, 2002, **47**, 3621–3628.
39 N. Lopez and F. Illas, *J. Phys. Chem. B*, 1998, **102**, 1430–1436.
40 S. Biing-Ming, S. Zhang and Z. C. Zhang, *J. Phys. Chem.*, 2004, **108**, 19510–19517.
41 B. O. Roos and K. P. Lawley, *Advances in Chemical Physics*, Wiley-Chichester, Inc., England, 1987.
42 J. S. Wilkes, *J. Mol. Catal. A: Chem.*, 2004, **214**, 11–17.
43 S. Zhang, X. Lu, Y. Zhang, Q. Zhou, J. Sun, L. Han, G. Yue, X. Liu, X. Cheng and S. Li, Springer-Verlag, 2008, DOI: 10.1007/430.
44 I. G. Cruz, D. Valencia, T. Klimova, R. O. Roa, J. M. Magadan, R. D. Balderas and F. Illas, *J. Mol. Catal. A: Chem.*, 2008, **281**, 79–84.
45 A. Ali, A. K. Nain and M. Kamil, *Thermochim. Acta*, 1996, **274**, 09–21.
46 S. G. Rao, T. M. Mohan, T. V. Krishna and B. S. Rao, *J. Chem. Thermodyn.*, 2016, **94**, 127–137.
47 M. T. Zafarani-Moattar and H. Shekaari, *J. Chem. Eng. Data*, 2005, **50**, 1694–1699.
48 E. J. González, B. González, N. Calvar and Á. Domínguez, *J. Chem. Eng. Data*, 2007, **52**, 1641–1648.
49 S. Bhagour, S. Solanki, N. Hooda, D. Sharma and V. K. Sharma, *J. Chem. Thermodyn.*, 2013, **60**, 76–86.
50 N. Deenadayalu, I. Bahadur and T. Hofman, *J. Chem. Thermodyn.*, 2010, **42**, 726–733.
51 N. Deenadayalu, I. Bahadur and T. Hofman, *J. Chem. Eng. Data*, 2010, **55**, 2636–2642.
52 N. Deenadayalu, I. Bahadur and T. Hofman, *J. Chem. Eng. Data*, 2011, **56**, 1682–1686.
53 I. Bahadur and N. Deenadayalu, *J. Solution Chem.*, 2011, **40**, 1528–1543.
54 I. Bahadur, N. Deenadayalu, Z. Tywabi, S. Sen and T. Hofman, *J. Chem. Thermodyn.*, 2012, **49**, 24–38.
55 I. Bahadur and N. Deenadayalu, *Thermochim. Acta*, 2013, **566**, 77–83.
56 I. Bahadur and N. Deenadayalu, *S. Afr. J. Chem.*, 2013, **66**, 200–206.
57 V. Govinda, P. M. Reddy, I. Bahadur, P. Attri, P. Venkatesu and P. Venkateswarlu, *Thermochim. Acta*, 2013, **556**, 75–88.
58 I. Bahadur, T. M. Letcher, S. Singh, G. G. Redhi, P. Venkatesu and D. Ramjugernath, *J. Chem. Thermodyn.*, 2015, **82**, 34–46.
59 S. Singh, I. Bahadur, G. G. Redhi, D. Ramjugernath and E. E. Ebenso, *J. Mol. Liq.*, 2014, **200**, 160–167.
60 S. Singh, I. Bahadur, G. G. Redhi, E. E. Ebenso and D. Ramjugernath, *J. Chem. Thermodyn.*, 2015, **89**, 104–111.
61 S. Singh, I. Bahadur, G. G. Redhi, E. E. Ebenso and D. Ramjugernath, *J. Mol. Liq.*, 2014, **199**, 518–523.
62 R. Gomes de Azevedo, J. M. S. S. Esperança and V. Najdanovic-Visak, *J. Chem. Eng. Data*, 2005, **50**, 997–1008.
63 M. T. Zafarani-Moattar and H. Shekaari, *J. Chem. Eng. Data*, 2005, **50**, 1694–1699.
64 Y. A. Sanmamed, D. González-Salgado, J. Troncoso, L. Romani, A. Baylaucq and C. Boned, *J. Chem. Thermodyn.*, 2010, **42**, 553–563.
65 E. Gómez, B. González, N. Calvar, E. Tojo and Á. Domìnguez, *J. Chem. Eng. Data*, 2006, **51**, 2096–2102.
66 K. Saravanakumar, R. B. Askran and T. R. Kubendran, *Asian J. Chem.*, 2011, **23**, 2643–2647.
67 T. J. Fortin, A. Laesecke, M. Freund and S. Outcalt, *J. Chem. Thermodyn.*, 2013, **57**, 276–285.
68 E. Cances, B. Mennucci and J. Tomasi, *J. Phys. Chem.*, 1997, **107**, 3032–3041.
69 J. P. Perdew, *Electronic Structure of Solids*, Akademie Verlag, Berlin, 1991, pp. 11–20.

70 K. Burke, J. P. Perdew and Y. Wang, *Electronic density functional theory: recent progress and new directions*, New York, 1998, p. 81.
71 R. Ditchfield, W. J. Hehre and J. A. Pople, *J. Chem. Phys.*, 1971, **542**, 724–728.
72 D. Singh, V. Singh, N. Islam and R. L. Gardas, *RSC Adv.*, 2016, **6**, 623–631.
73 V. H. Álvarez, D. Serrão, J. L. da Silva Jr, M. R. Barbosa and M. Aznar, *Ionics*, 2013, **19**, 1263–1269.
74 D. Keshapolla and R. L. Gardas, *Fluid Phase Equilib.*, 2014, **383**, 32–42.
75 B. A Marekha, M. Bria, M. Moreau, I. De Waele, F.-A. Miannay, Y. Smortsova, T. Takamuku, O. N. Kalugin, M. Kiselev and A. Idrissi, *J. Mol. Liq.*, 2015, **210**, 227–237.
76 M. J. Frisch, G. W. Trucks, H. B. Schlegel, G. E. Scuseria, M. A. Robb, J. R. Cheeseman, G. Scalmani, V. Barone, B. Mennucci, G. A. Petersson, H. Nakatsuji, M. Caricato, X. Li, H. P. Hratchian, A. F. Izmaylov, J. Bloino, G. Zheng, J. L. Sonnenberg, M. Hada, M. Ehara, K. Toyota, R. Fukuda, J. Hasegawa, M. Ishida, T. Nakajima, Y. Honda, O. Kitao, H. Nakai, T. Vreven, J. A. Montgomery Jr, J. E. Peralta, F. Ogliaro, M. Bearpark, J. J. Heyd, E. Brothers, K. N. Kudin, V. N. Staroverov, T. Keith, R. Kobayashi, J. Normand, K. Raghavachari, A. Rendell, J. C. Burant, S. S. Iyengar, J. Tomasi, M. Cossi, N. Rega, J. M. Millam, M. Klene, J. E. Knox, J. B. Cross, V. Bakken, C. Adamo, J. Jaramillo, R. Gomperts, R. E. Stratmann, O. Yazyev, A. J. Austin, R. Cammi, C. Pomelli, J. W. Ochterski, R. L. Martin, K. Morokuma, V. G. Zakrzewski, G. A. Voth, P. Salvador, J. J. Dannenberg, S. Dapprich, A. D. Daniels, O. Farkas, J. B. Foresman, J. V. Ortiz, J. Cioslowski and D. J. Fox, *G09a: GAUSSIAN 09, Revision B.01*, Gaussian, Inc., Wallingford CT, 2010.
77 J. A. Riddick, W. B. Bunger and T. K. Sakano, *Organic solvents*, Wiley-Interscience, New York, 4th edn, 1986.
78 C. Kolbeck, J. Lehmann, K. R. J. Lovelock, T. Cremer, N. Paape, P. Wasserscheid, A. P. Fröba, F. Maier and H.-P. Steinrück, *J. Phys. Chem. B*, 2010, **114**, 17025–17036.
79 Y. T. Wang and G. A. Voth, *J. Am. Chem. Soc.*, 2005, **127**, 12192–12193.
80 J. N. A. C. Lopes and A. A. H. Pádua, *J. Phys. Chem. B*, 2006, **110**, 3330–3335.
81 V. Govinda, P. Venkatesu and I. Bahadur, *Phys. Chem. Chem. Phys.*, 2016, **18**, 8278–8326.
82 O. Redlich and A. Kister, *Ind. Eng. Chem.*, 1948, **40**, 345–348.
83 M. M. Taib and T. Murugesan, *J. Chem. Eng. Data*, 2012, **57**, 120–126.
84 L. Cammarata, S. G. Kazarian, P. A. Salterb and T. Welton, *Phys. Chem. Chem. Phys.*, 2001, **3**, 5192–5200.
85 M. A. Iglesias-Otero, J. Troncoso, E. Carballo and L. Romani, *J. Chem. Thermodyn.*, 2008, **40**, 949–956.
86 M. Anouti, A. Vigeant, J. Jacquemin, C. Brigouleix and D. Lemordant, *J. Chem. Thermodyn.*, 2010, **42**, 834–845.
87 Y. Tian, X. Wang and J. Wang, *J. Chem. Eng. Data*, 2008, **53**, 2056–2059.
88 I. M. Alecu, J. Zheng, Y. Zhao and D. G. Truhlar, *J. Chem. Theory Comput.*, 2010, **6**, 2872–2887.
89 N. Cheng, P. Yu, T. Wang, X. Sheng, Y. Bi, Y. Gong and L. Yu, *J. Phys. Chem. B*, 2014, **118**, 2758–2768.
90 W. Xu, T. Wang, N. Cheng, Q. Hu, Y. Bi, Y. Gong and L. Yu, *Langmuir*, 2015, **31**, 1272–1282.
91 Y. Zhao, J. Wang, H. Wang, Z. Li, X. Liu and S. Zhang, *J. Phys. Chem. B*, 2015, **119**, 6686–6695.
92 M. Bešter-Rogač, A. Stoppa and R. Buchner, *J. Phys. Chem. B*, 2014, **118**, 1426–1435.